JOURNAL OF CATALYSIS 47, 147–158 (1977)

Symmetries of the Oxygen Ligands of Ni(II) and Co(II) Ions in Synthetic A, X, and Y Zeolites

JANUSZ M. JABŁOŃSKI, JACEK MULAK, AND WŁADYSŁAW ROMANOWSKI

Institute for Low Temperature and Structure Research, Polish Academy of Sciences,
Plac Katedralny 1, P.O. Box 937, 50-950 Wroclaw, Poland

Received June 2, 1975; revised December 18, 1975

The magnetic susceptibility of Ni^{2+} and Co^{2+} ions in fully and partly dehydrated X, Y, and A zeolites has been measured over the temperature range from 4.2 to 300 K. Zeolites of various exchange levels (11–69%) have been investigated.

A comparison of ionic radii of Ni^{2+}, Co^{2+}, and of O^{2-} shows that Ni^{2+} and Co^{2+} ions in dehydrated zeolites can assume C_{3v} and C_{4v} symmetries as well as the previously proposed (*11, 12*) O_h and T_d coordinations. The temperature dependences of the magnetic susceptibility of Ni^{2+} and Co^{2+} in C_{3v} and C_{4v} O^{2-} ligand symmetries were calculated from crystal field theory, using Van Vleck's formula. By comparison of the experimentally found $\chi_M(T)$ dependences with those theoretically calculated for C_{3v} and C_{4v}, as well as with those already known for O_h and T_d symmetries, we have tried to determine a sequence of occupation and distribution of Ni^{2+}, Co^{2+} ions in zeolites as depending on temperature, dehydration time and dehydration level. It was established that in fully dehydrated Y zeolite there is a preference for Ni^{2+} ions to occupy C_{4v} sites and for Co^{2+} to occupy C_{3v} sites, whereas in X and A zeolites no such preference to occupy specific sites is found. No relation between the quantity of exchanged ions and distribution or sequence of occupation of exchange positions seems to exist for A and X zeolites.

In partly dehydrated zeolites the change of the $\chi_M^{-1}(T)$ slope with the degree of dehydration is similar to that described in other papers. It seems that the main factors controlling the process of occupation and distribution of the ion exchange sites are the parameters of the dehydration process and ion migration in the zeolites.

In fully dehydrated zeolites the exchange sites of low coordination number and C_{3v} or C_{4v} symmetries are most probable on geometrical, electrostatic and chemical grounds.

INTRODUCTION

Extensive application of zeolites as catalysts and adsorbents has prompted also the development of basic studies of their physicochemical and structural properties. By the application of X-ray structure analysis (*1–4*), electron resonance (*5–7*), reflectance spectroscopy (*5, 8–10*) and magnetic studies (*11–13*), the structure of the aluminosilicate framework of zeolites has been established and information obtained on the coordination and location of transition metal ions compensating the excess charge of the framework. Each of these techniques has its limitations and does not allow one to solve the problem completely.

In the present work we have applied the magnetic susceptibility method to find the symmetries of the surroundings of Ni^{2+} and Co^{2+} ions in synthetic zeolites. The method consists in comparing the experimentally found (χ_M^{-1},T) relations with those expected theoretically for models with different symmetries of coordination of the paramagnetic ions.

Egerton *et al.* (*11, 12*), using the change of the (χ_M^{-1},T) plots during dehydration of X, Y, and A zeolites, have found rela-

ISSN 0021-9517

tions between the symmetry of the Ni^{2+} and Co^{2+} ion environments in these zeolites and their degree of hydration. They assumed only octahedral and tetrahedral coordinations of the paramagnetic ions in fully or partly hydrated zeolites, which certainly does not suffice in the case of complete dehydration. The coordinations of C_{3v} or C_{4v} for A zeolites and those of C_{3v}, C_{4v} or O_h symmetries for X and Y zeolites have been assumed in the present paper as the basic ones in their fully dehydrated forms.

EXPERIMENTAL METHODS

Y and A zeolites produced by Union Carbide and labeled as SK-40 and A5, and X-13 zeolite from the Inowrocław Soda Factory, Poland were used.

The granulated SK-40 zeolite was crushed and separated into two fractions, namely, below 0.25 mm and from 0.25 to 0.75 mm, and washed with distilled water before the ion exchange. No significant differences in the extent of exchange at the given conditions and in the magnetic properties of the exchanged ions have been established among the fractions in careful, separate experiments. We used the 0.25–0.75 mm fractions for the sake of convenience (no clogging of the small passages and no adhesion to the glass walls in the course of dehydration under vacuum).

The other material (A and X) was in the form of the powder without binder. We used it in this form during the whole course of experiments, regardless of its being more difficult to handle during the dehydration and transfer under vacuum.

The process of ion exchange was carried out at room temperature in occasionally stirred aqueous solutions of nickel and cobalt acetates. The pH of the solutions was equal to ca. 6. The nickel and cobalt contents were determined gravimetrically via complexes with dimethylglyoxime and α-nitro-β-naphthol, respectively, and are given as weight percent and as the exchange degree of Na^+ cations. Fifteen different samples of nickel- and 16 samples of cobalt-exchanged zeolites were investigated and their characteristics are given in Table 1.

The process of dehydration and outgassing of the samples was carried out in three stages in a conventional vacuum apparatus. After an initial outgassing at room temperature the samples were slowly heated during 4 to 8 hr to 430°C under dynamic vacuum. The final dehydration and outgassing proceeded during 5 or 10 hr of heating at 430°C in a vacuum of 10^{-5} mm Hg. To avoid possible reduction of metal ions in the zeolite by grease vapors, a liquid nitrogen trap was installed directly before the sample. Samples for the magnetic measurements weighed about 400 mg and were sealed off *in vacuo* into ball-shaped glass containers of ca. 8 mm diameter. The measurements of the magnetic susceptibility were carried out by the Faraday method within the temperature ranges of 4–300 K or 77–300 K. The measurements within the range 4–300 K were carried out under a helium atmosphere (5 mm Hg) in a tightly closed Cahn microbalance and the measurements at 77–300 K on a standard apparatus in a hydrogen atmosphere. The magnetic susceptibility was measured at five different field intensities up to 6700 Oe. Calibration of the magnetic field intensity H and of its gradient $\partial H/\partial x$ was performed by means of Mohr salt and mercury tetrathiocyanato-cobaltate as standard substances with precisely known magnetic susceptibility. The corrections for the magnetic susceptibility of unexchanged, parent zeolites were also found experimentally for all magnetic field intensities used and for the whole temperature range. Temperature functions of the gram susceptibility for the three types of zeolites are presented in Fig. 1. Unexchanged zeolites are characterized by positive values of susceptibility, which, as indicated by the straight line dependence of susceptibility on field strength, are due to

TABLE 1

Magnetic Properties of Fully Dehydrated Nickel- and Cobalt Exchanged Zeolites

No.	Zeolite	Nickel content (wt%)	μ [μ_B]	θ [K]	No.	Zeolite	Cobalt content (wt%)	μ [μ_B]	θ [K]
1	NiY 11.5[a]	1.44	4.20	−30	1	CoY 23.9	3.00	4.90	−30
2	NiY 25.5	3.20	4.44	−43	2	CoY 27.0	3.40	5.90	−47
3	NiY 38.8	4.86	3.68	−15	3	CoY 38.6	4.85	5.28	−35
4	NiY 43.6	5.46	3.48	0	4	CoY 57.3	7.20	5.70	−47
5	NiY 43.6[b]	5.46	3.76	−11	5	CoY 59.5	7.46	5.70	−38
6	NiY 52.7	6.60	3.92	−25	6	CoY 59.8	7.55	4.90	0
7	NiY 53.5	6.70	4.47	−45	7	CoY 68.4	8.57	4.90	−15
8	NiY 53.5	6.70	3.59	−2	8	CoY 68.4[b]	8.57	4.90	−8
9	NiY 54.5	6.85	4.40	−37					
10	NiY 57.1	7.15	3.68	0					
11	NiY 57.1	7.15	3.57	0					
12	NiX 20.4	3.75	3.58	−10	9	CoX 12.6	2.33	4.67	−22
13	NiX 20.4	3.75	3.40	−13	10	CoX 26.0	4.80	4.55	−2
14	NiX 23.9	4.40	3.83	−16	11	CoX 51.0	9.43	4.70	−22
15	NiX 35.6	6.56	3.71	−12	12	CoX 54.7	10.10	4.70	−1
16	NiX 45.5	8.40	3.57	0	13	CoX 54.7	10.10	5.25	−8
17	NiX 45.5	8.40	3.56	0	14	CoX 63.9	11.70	4.65	−20
18	NiX 45.5[b]	8.40	3.60	−5	15	CoX 63.9[b]	11.70	5.02	−13
19	NiX 55.4	10.20	3.24	0	16	CoX 65.5	12.10	5.26	−18
20	NiA 16.4[b]	3.25	3.65	−8	17	CoA 21.2[b]	4.20	4.23	−33
21	NiA 21.3[b]	4.20	3.54	−13	18	CoA 31.3[b]	6.20	4.57	−37

[a] NiY 11.5, etc., denote samples in which 11.5% Na$^+$ ions have been replaced by Ni, etc. . . .

[b] Denotes samples dehydrated during 10 hr at 430°C (see text).

paramagnetic impurities, mainly Fe [see also (*11*)]. The corrections thus arising are not negligible, especially for low levels of exchange and at higher temperatures. At liquid helium temperature they reach 18 × 10^{-6} emu, whereas at room temperature they amount to ca. 1 × 10^{-6} emu. As a rule, however, the value of the correction did not exceed 10% of the total susceptibility measured for the exchanged zeolites. The corrections for diamagnetism of the paramagnetic ions were neglected, as they are much smaller than the experimental error of measurement.

RESULTS

Specifications of the measured samples, and their exchange degrees together with the Curie–Weiss parameters of their paramagnetic susceptibilities are given in Table 1. Typical experimental plots of magnetic susceptibility vs temperature for three nickel- and cobalt-exchanged zeolites are shown in Figs. 2 and 3. Theoretically cal-

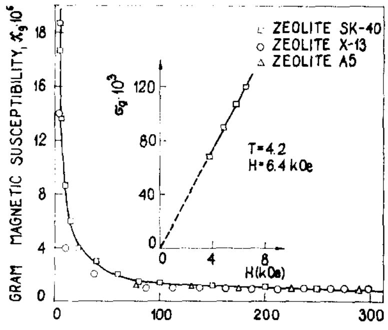

Fig. 1. Gram magnetic susceptibility of fully dehydrated X, Y, and A parent zeolites.

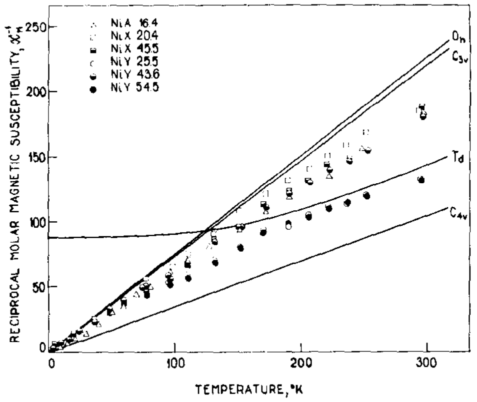

FIG. 2. Reciprocal susceptibility of Ni^{2+} ions in fully dehydrated X, Y, and A zeolites as a function of temperature at different exchange levels.

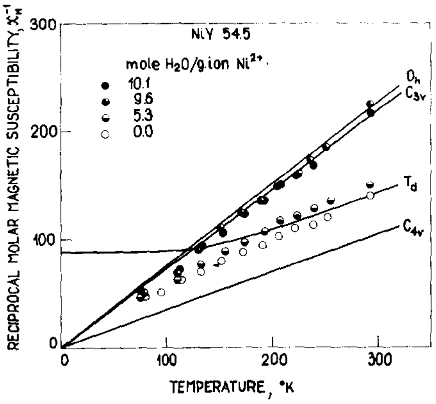

FIG. 4. Reciprocal susceptibility of NiY 54.5 as a function of temperature at different degrees of hydration.

culated functions of reciprocal molar susceptibility vs temperature (see Appendix) are shown by solid lines. To check the repeatability of the dehydration process and that of the magnetic measurements, some samples were prepared and examined twice (Table 1). Considering the substantial changes in symmetry of Ni^{2+} and Co^{2+} coordinations with the hydration degree of zeolite (*11*, *12*), susceptibility measurements of differently hydrated samples were also performed. By way of example, Figures 4 and 5 show such courses for selected nickel and cobalt zeolites against a background of four theoretical plots. The poor reproducibility of the (χ_M^{-1}, T) experimental plots for identical samples dehydrated under approximately the same conditions is illustrated in Fig. 6 and in Table 1.

The experimental temperature functions of magnetic susceptibility obey the Curie–Weiss law only roughly. This is rather easily understandable in the light of the general Van Vleck expression for the paramagnetic susceptibility of non-free ions. Deviation of the (χ_M^{-1}, T) plots from a straight line and occurrence of θ constant results directly from the Van Vleck formula, and cannot be a priori related to exchange

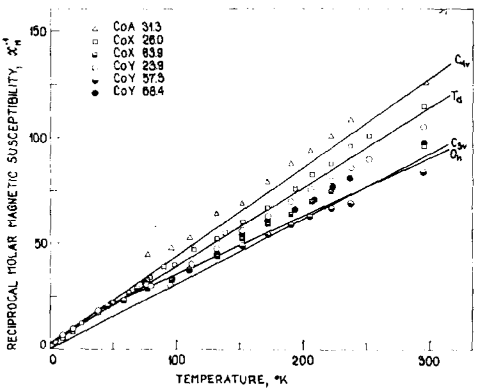

FIG. 3. Reciprocal susceptibility of Co^{2+} ions in fully dehydrated X, Y, and A zeolites as a function of temperature at different exchange levels.

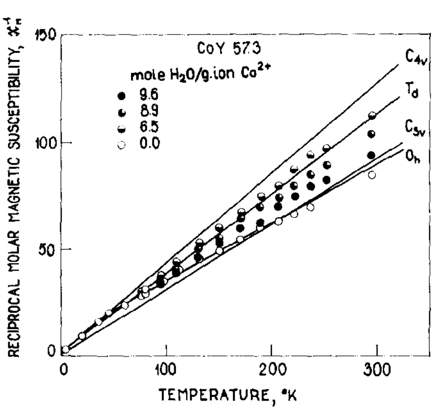

FIG. 5. Reciprocal susceptibility of CoY 57.3 as a function of temperature at different degrees of hydration.

interactions between the paramagnetic ions. In Table 1 and in all the figures, experimental values of the susceptibility are given neglecting possible exchange interactions. Taking into account the magnetic dilution of the transition metal ions in zeolite, as well as the "loose" structure which decrease both the exchange and superexchange interactions, we regard the definition of the corrected paramagnetic susceptibility as $(\chi_M^{-1})_{\mathrm{corr}} = (\chi_M^{-1})_{\mathrm{exp}} - \lambda$, where $\lambda = \theta/C$ (*11*, *12*) as unwarranted.

No explicit correlation between the exchange degree and values of the magnetic moment and hence the sequence and distribution of exchange sites in zeolites seems to result from the data of Table 1 and Figs. 2 and 3. However, some differences between the zeolites X, A and Y may be observed. The magnetic moment of the Ni^{2+} ion in Y zeolite attains higher values than for X and A zeolites. Its maximum value approaches 4.5 μ_B, which corresponds to the preference of occupying of C_{4v} (4.77 μ_B) or T_d symmetry sites. The values of the magnetic moment of Ni^{2+} ions in X and A zeolites, fluctuating within the range of 3.2–3.8 μ_B, are close to the average value for several different coordinations of the Ni^{2+} ion, which indicates that none of them is preferential. The assumption of tetrahedral symmetry for the Ni^{2+} ion environment in the A zeolite is clearly at variance with the experimental (χ_M^{-1}, T) plots. While the theoretically expected susceptibility for T_d symmetry is roughly temperature independent up to ca. 150 K, the experimental plots conform to the Curie–Weiss law with a magnetic moment of ca. 3.6 μ_B and the θ constant being close to zero. Therefore, one may presume that perfect tetrahedral coordination of Ni^{2+} ions in the A zeolite does not occur. This conclusion may be generalized for the other types of zeolites.

In the case of cobalt-exchanged zeolites (Fig. 3) one also observes some differences in (χ_M^{-1}, T) plots according to the kind of zeolite. However, unlike the previous case, the magnetic moment of the Co^{2+} ion in the Y zeolite, being higher than those for the X and A zeolites, indicates some preference in occupying C_{3v} or O_h symmetry sites. A considerable divergence of (χ_M^{-1}, T) plots for similar exchange levels, as well as a coincidence of values of the magnetic moment for different types of zeolites, do not allow us to establish the actual occupation of exchange sites and their distribution as dependent on the type of zeolite.

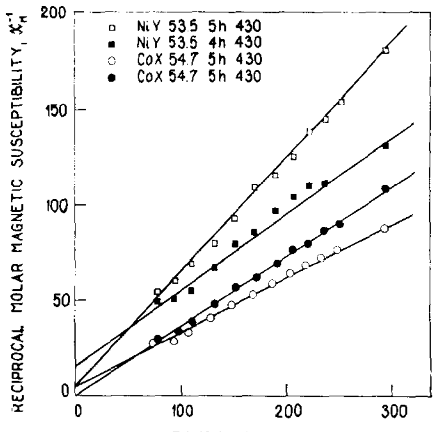

FIG. 6. Divergence of (χ_M^{-1}, T) plots for NiY 53.5 and CoX 54.7 dehydrated under approximately the same conditions.

Figures 4 and 5 show the (χ_M^{-1}, T) plots for nickel- and cobalt-exchanged Y zeolite for four different degrees of hydration, which are illustrative of changes of the magnetic moment during the dehydration process. The magnetic moment of NiY samples rises gradually from 3.2 up to 4.4 μ_B upon dehydration. In the case of CoY zeolite, the magnetic moment drops from 5.2 to 4.6 μ_B at the first stage of dehydration, but at the final stage it again increases, for some samples even to 5.7 μ_B. The observed changes of the magnetic susceptibility and moment are qualitatively consistent with those obtained in previous works (*11*, *12*).

However, in the light of the results obtained for a larger number of dehydrated samples, the above findings may be considered only as tendencies of changes of the magnetic susceptibility and moment during dehydration. A review of our extensive experimental material on zeolites exchanged and hydrated in different degrees, as well as dehydrated under various conditions, gives no evidence for a distinct correlation between these parameters and the coordination symmetry of the paramagnetic cations in a zeolite. An example of this is the (χ_M^{-1}, T) plots for two pairs of identical NiY and CoY samples dehydrated approximately under the same conditions (Fig. 6).

DISCUSSION

According to the results of X-ray investigations of dehydrated X and Y zeolites, the cations may be introduced into three types of exchange sites. These are (*14*, *15*): I, sites within the hexagonal prisms (16/unit cell); II, sites at the hexagonal windows slightly shifted towards the supercage (32/unit cell); and I′, II′, sites within the sodalite units (32/unit cell each). The ocsupation of the sites III (48/unit cell), cituated within the supercage, seems to be also possible. For steric and electrostatic reasons the occupying of the sites designated as U, V, and II* is unlikely. These sites may be of importance in fully or partly hydrated zeolites only, provided that the "location" of hydrated ions in zeolite makes sense at all. The simultaneous presence of cations in sites II and II′ at the the same hexagonal window is out of the question in view of the small distance and strong electrostatic repulsion between them. The simultaneous occupation of the I and I′ sites seems to be similarly excluded, whereas the occupying of III sites is free from such restrictions. There are no I and I′ sites in dehydrated A zeolites. Here, the sites analogous to those of II and II′ types in the X or Y zeolites, as well as those at the centers of eight-membered rings, are occupied (*16*). The sites lying on both sides of the D_4 ring, within the supercage or within the sodalite cell, are probably also occupied. Similarly, III, U and V sites cannot occur in the dehydrated A zeolite. In the X and A zeolites, with their ratio of Si/Al close to 1, there is only one kind of six-membered rings composed of tetrahedra SiO_4^{4-} and AlO_4^{5-}, arranged alternatively. In the Y zeolites, for which the ratio of Si/Al ≈ 2.5, various kinds of arrangement of Si and Al tetrahedra in the ring may occur (*5*). Because of this arrangement of the tetrahedra and the electrostatic requirements resulting from it, the most privileged sites in the X and A zeolites are those of maximum density of uncompensated charge, i.e., the sites designated as I, I′, II, II′, and II, II′, respectively.

In the Y zeolites, on account of the lack of any close range ordering of Si and Al tetrahedra, the charge distribution in the aluminosilicate framework is rather random and the other sites may be preferred. Olson (*2*), and Gallezot and Imelik (*3*) showed by means of X-ray analysis that in fully dehydrated Y zeolite the Ni^{2+} ions are located mainly in the I and II sites. However, the limitations of the X-ray methods do not allow one to locate all the Ni^{2+} ions. Probably, the unidentified ions occupy the sites at the walls of the supercage (*3*). Co^{2+} ions in the A zeolites go into the II′-like sites, i.e., those lying on the 3-fold axis in the vicinity of the six-membered oxygen windows, a little inwards of the sodalite cell (*4*). The above conclusions have been confirmed by the results of electron resonance and reflectance spectroscopy studies (*5*, *6*, *8–10*).

According to the results of the above investigations, Ni^{2+} and Co^{2+} ions in the X and Y zeolites occupy first of all the I sites, reaching almost perfect octahedral environment, as well as the II and II′ sites, in which the C_{3v} coordinations by three oxygen anions from the framework may be completed to the distorted T_d coordination by addition of a fragment of a water molecule: OH^- or even O^{2-}. Owing to the absence of the I sites in the A zeolites, the exchanged ions can occupy the II and II′ sites only.

The work of Gallei *et al.* (*17*) on the ion exchange of zeolites in water solutions at room temperature shows that the ions forming hexahydrates are present within the supercage only, because of the steric hindrance they cannot penetrate into the sodalite cage (I′ and II′ sites) and into the hexagonal prism (I sites). Thus it follows that during and after the dehydration process the ions, being gradually stripped of their hydration shell, migrate to the new sites which are unattainable for them in the hydrated state. Therefore, the distribution of the occupied exchange sites may strongly depend on the kinetics of the dehydration and migration of the ions.

On the basis of our present results some additional rules may be formulated about the occupation of various sites by Ni^{2+} and Co^{2+} ions in A, X, and Y zeolites. In the fully dehydrated zeolites it is rather improbable for the transition metal ions to occupy the sites of higher symmetry of environment O_h, T_d. It follows both from the comparison of ionic radii of the exchanged cations and that of the O^{2-} anion and from the rigidity of the aluminosilicate framework. Additionally, some directive character of the covalent part of the Me–O bonds and polarizing effects, modifying the effective electrostatic charges may also play a role. It should be emphasized here that the properties of exchanged paramagnetic ions are determined by the symmetry of the electrostatic field rather than by geometric symmetry.

Localization of the anhydrous Ni^{2+} and Co^{2+} cations in sites far removed from the walls of zeolite framework and not ensuring contact between the cations and O^{2-} anions is impossible from the electrostatic point of view. The polarization of the environment by the metal cation cannot be too strong with regard to the stability of SiO_4^{4-} and AlO_4^{5-} tetrahedra. Therefore, it seems to be improbable for a cation with a radius equal to 0.7 Å to occupy the sites I′, II′, or II lying at the center of the six-membered oxygen window with the diameter of ca. 2.4 Å, as well as the I sites in the center of the hexagonal prism, composed of two such six-membered rings. When the dehydrated Ni^{2+} and Co^{2+} cations enter the hexagonal prism, they are shifted towards the walls of the zeolite framework. Thus the actual coordination numbers within the first sphere become lower and C_{3v} or C_{4v} point symmetry should prevail. Both Egerton *et al.* (*11*) and Olson (*2*) seem to have disregarded such simple electrostatic arguments and proposed the Ni^{2+} or Co^{2+} cations to stay "suspended" in the center of the hexagonal prism between six equally distant, oxygen ions. The model of Olson is based on average Ni–O distances obtained from X-ray analysis and requires considerable (about 0.5 Å) shift of the O(3) oxygen toward the Ni cation (as compared with the nonexchanged faujasite). This is too big a deformation to be assumed in the otherwise rigid Si–Al framework. On the other hand, the course of the magnetic susceptibility with temperature also does not allow us to distinguish between C_{3v} and O_h positions (see Figs. 2 and 3). So the accurate position of Ni^{2+} and Co^{2+} ions in the hexagonal prism remains uncertain, since both X-ray and crystal field methods are not capable of determining them with the required accuracy.

The heterogeneity of the distribution of uncompensated electrostatic charge in the Y zeolite is presumably responsible for the noticeable tendency for sites of one type to be occupied in this zeolite, contrary to the lack of any preferences in the case of the X and A zeolites. The sites of C_{4v} symmetry in the case of the Ni^{2+} ion, and those of C_{3v} symmetry in the case of the Co^{2+} ion, are the distinguished ones in the Y zeolite. The tendency of the Ni^{2+} ion to assume C_{4v} coordination corresponds to its preference to form square-planar complexes with coordination number 4 while this configuration is not frequently encountered with Co^{2+}.

There remains still the question of the poor reproducibility of the magnetic properties of samples dehydrated approximately in the same way. From the papers published before (*8*, *11*, *12*) it follows that the temperature of 400–430°C and high vacuum is sufficient for complete dehydration. In our experiments we established that our procedure resulted in a weight loss of about 27%, which corresponds to complete dehydration. However, from the previous investigations (*18*) it is clear that a certain amount of OH^- ions associated with the exchanged cations remains in the lattice at that temperature, which certainly influences the symmetry of the possible environment of these cations.

The complete removal of H_2O is probably not a sufficient condition for attaining equilibrium distribution of the exchanged cations. The processes of dehydration and of migration can, and probably do, proceed at different rates, and some exchanged ions can be "trapped" at nonequilibrium positions at the end of H_2O removal. In such a situation one cannot expect the nonequilibrium distribution to be the same in each of consecutive experiments, when the treatment is only approximately the same and difficult to control. There seems to have been little attention paid to this problem and no attempts to control carefully the factors influencing the kinetics of dehydration and to attain true equilibrium positions of the cations have ever been made.

CONCLUSIONS

The present results show that the finding of the coordination symmetry of paramagnetic ions in zeolites based on magnetic data is impeded both by the occurrence of mixed occupation and by the coincidence of the temperature functions of the magnetic susceptibility for different symmetries. In the fully dehydrated zeolites, the Ni^{2+} and Co^{2+} ions have at their disposal several different sites. For geometric, electrostatic and chemical reasons, the most preferred sites are those with coordination number of 3 or 4 and C_{3v} or C_{4v} point symmetry of environment.

The use of the magnetic method does not allow us to define any distinct correlation explaining the sequence of occupying of the exchange sites and their distribution. Physical parameters of the dehydration and the process of ion migration seem to be the crucial factors of the process of occupation of the exchange sites in zeolite. The ambiguity of results concerning the location of transition metal ions in synthetic zeolites is characteristic not only for the magnetic method described above. Unfortunately, all methods used so far, except maybe for some special cases, give results "averaged" in some unknown way over all possible exchange sites.

APPENDIX

ELECTRONIC GROUND STATE AND TEMPERATURE FUNCTION OF PARAMAGNETIC SUSCEPTIBILITY OF Ni^{2+} AND Co^{2+} IONS OCCUPYING C_{3v}, C_{4v}, O_h AND T_d POINT SYMMETRY SITES IN ZEOLITES

Comparison of the ionic radii of anhydrous cations [Ni^{2+} (0.69 Å), Co^{2+} (0.72 Å), and oxygen anion O^{2-} (1.40 Å)] leads to the supposition that the most probable exchange sites on the framework of O^{2-} anions are those of C_{3v} and C_{4v} point symmetry (Fig. 7).

Based on the hard sphere and point charge models, the Hamiltonian of the electrostatic crystal field, produced by the given configurations of O^{2-} anions in the space around the paramagnetic ion, has been defined and calculated. Electron eigenstates and eigenvalues of Ni^{2+} and Co^{2+} ions have been found by simultaneous diagonalization of the matrix of crystal field interaction and spin–orbit coupling, i.e., the matrix of the Hamiltonian:

$$H = H_{\mathrm{cf}} + H_{LS}. \qquad (1)$$

The values of the parameters of the electronic structure of Ni^{2+} and Co^{2+} ions used in the calculations are presented in Table 2. The point charge model gives the following expressions for the crystal field Hamiltonians:

$$H_{\mathrm{cf}}{}^{\mathrm{Ni}(3v)} = 23\hat{\mathrm{O}}_2{}^0 - 1.4\hat{\mathrm{O}}_4{}^0 + 33.5\hat{\mathrm{O}}_4{}^3, \qquad (2)$$

$$H_{\mathrm{cf}}{}^{\mathrm{Ni}(4v)} = -106\hat{\mathrm{O}}_2{}^0 + 0.1\hat{\mathrm{O}}_4{}^0 + 15.3\hat{\mathrm{O}}_4{}^4, \qquad (3)$$

$$H_{\mathrm{cf}}{}^{\mathrm{Co}(3v)} = -31\hat{\mathrm{O}}_2{}^0 + 1.6\hat{\mathrm{O}}_4{}^0 - 37.4\hat{\mathrm{O}}_4{}^3, \qquad (4)$$

$$H_{\mathrm{cf}}{}^{\mathrm{Co}(4v)} = 100\hat{\mathrm{O}}_2{}^0 + 0.2\hat{\mathrm{O}}_4{}^0 - 16.5\hat{\mathrm{O}}_4{}^4, \qquad (5)$$

where:

$$\begin{aligned}
\hat{\mathrm{O}}_2{}^0 &= 3\hat{L}_z{}^2 - 12,\\
\hat{\mathrm{O}}_4{}^0 &= 35\hat{L}_z{}^4 - 335\hat{L}_z{}^2 + 360,\\
\hat{\mathrm{O}}_4{}^3 &= \hat{L}_z(\hat{L}_+{}^3 + \hat{L}_-{}^3) + (\hat{L}_+{}^3 + \hat{L}_-{}^3)\hat{L}_z,\\
\hat{\mathrm{O}}_4{}^4 &= \hat{L}_+{}^4 + \hat{L}_-{}^4.
\end{aligned}$$

The coefficients at the equivalent operators $\hat{\mathrm{O}}_n{}^m$ are given in cm^{-1}. The spin–orbit coupling Hamiltonian has the form:

$$H_{LS} = \lambda[\hat{L}_z\hat{S}_z + \tfrac{1}{2}(\hat{L}_+\hat{S}_- + \hat{L}_-\hat{S}_+)]. \qquad (6)$$

TABLE 2

Electronic Parameters of Ni^{2+} and Co^{2+} Ions

	Ni^{2+}	Co^{2+}
Configuration	$3d^8$	$3d^7$
Ground term	^3F	^4F
Ground term degeneracy	21	28
λ [cm^{-1}]	−300	−150
$\langle r^2\rangle$ [a.u.]	1.13	1.25
$\langle r^4\rangle$ [a.u.]	3.00	3.66
α	2/105	−2/105
β	2/315	−2/315

The basis of initial (zero approximation) wave functions $|LSL_zS_z\rangle$ consists of 21 and 28 vectors for Ni^{2+} and Co^{2+} ions, respectively. The 21st order matrices of the Hamiltonians (2) + (6) and (3) + (6) may be reduced to the block forms: (5 × 5) + 2(5 × 5) + (6 × 6) and 2(7 × 7) + (7 × 7), respectively. Similarly, the 28th order matrices of the Hamiltonians (4) + (6) and (5) + (6) are reducible to the block forms: 2(7 × 7) + 2(7 × 7) and 2(9 × 9) + (10 × 10), respectively. However, the crystal field Hamiltonian calculated from the point charge model does not in general correspond to the real one. Its various potential terms are lowered several times and to different extents. Therefore, the real composition of the ground state has been found by analysis of four variants, the second order term of the potential being enlarged 1, 1, 2 and 3 times, and the fourth order terms 1, 3, 5, and 10 times respectively, with the parameter λ held constant. The magnitudes of the total splitting of the ground terms and the values of the g factor indicate that a satisfactory agreement with the experiment may be obtained by multiplying the second order term of the potential 2 to 3 times, and the fourth order terms 5 to 10 times. The variants considered above do not differ essentially with respect to the ground state and this allows its average, representative composition to be defined.

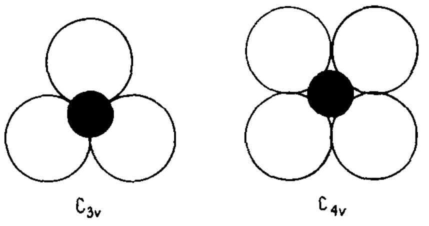

FIG. 7. C_{3v} and C_{4v} coordinations of Ni^{2+} or Co^{2+} cations by O^{2-} anions of zeolite framework (to scale).

The level system comprising the Boltzmann population up to 300 K has been assumed to be a ground state. The averaged ground states, accurate to the component wave functions, whose contribution is above 1%, are given below.

Ni^{2+}, C_{3v}

An isolated pseudotriplet (doublet + singlet) with zero splitting of few cm^{-1} is the ground state. It has the form:

$$\begin{array}{cl}
\left\{\begin{array}{c}—\\—\end{array}\right\} & \begin{array}{l} -0.78|0\bar{1}\rangle + 0.48|\bar{3}\bar{1}\rangle - 0.38|3\bar{1}\rangle - 0.10|\bar{1}0\rangle \\ 0.78|01\rangle + 0.48|31\rangle - 0.38|\bar{3}1\rangle + 0.10|10\rangle \end{array} \\
— & 0.78|00\rangle + 0.43|30\rangle - 0.43|\bar{3}0\rangle + 0.10|\bar{1}1\rangle + 0.10|1\bar{1}\rangle,
\end{array}$$

and its paramagnetic susceptibility is equal to:

$$\chi_M = \frac{N\mu_B^2}{3kT}(10.74) = \frac{1.34}{T},$$

with an effective moment of 3.28 μ_B.

Ni^{2+}, C_{4v}

There are five close lying levels (a doublet + 3 singlets) within the thermal population at the room temperature. Their total span does not exceed 500 K.

$$\begin{array}{cl}
— & -0.60|20\rangle + 0.60|\bar{2}0\rangle - 0.29|3\bar{1}\rangle + 0.29|\bar{3}1\rangle - 0.20|11\rangle + 0.20|\bar{1}\bar{1}\rangle \\
\left\{\begin{array}{c}—\\—\end{array}\right\} & \begin{array}{l} -0.60|\bar{2}\bar{1}\rangle + 0.55|2\bar{1}\rangle - 0.50|\bar{3}0\rangle + 0.30|10\rangle \\ -0.60|21\rangle + 0.55|\bar{2}1\rangle - 0.50|30\rangle + 0.30|\bar{1}0\rangle \end{array} \\
— & 0.63|31\rangle - 0.63|\bar{3}\bar{1}\rangle - 0.32|\bar{1}1\rangle + 0.32|1\bar{1}\rangle \\
— & 0.63|31\rangle + 0.63|\bar{3}\bar{1}\rangle - 0.32|\bar{1}1\rangle - 0.32|1\bar{1}\rangle.
\end{array}$$

Assuming their degeneracy, one obtains the following formula for the paramagnetic susceptibility:

$$\chi_M = \frac{N\mu_B^2}{3kT}(22.80) = \frac{2.85}{T},$$

corresponding to an effective moment of 4.77 μ_B.

The fine structure of the ground state affects the temperature function of the susceptibility only slightly and only at low temperatures. The singlet ground level is connected with the occurrence of a certain range of temperature-independent paramagnetism; the approximate Curie–Weiss (χ_M^{-1}, T) plot then usually gives a θ constant different from zero.

Co^{2+}, C_{3v}

Four approximately equidistant Kramers doublets separated by gaps of ca. 360 K lie within the range of thermal population at 300 K:

$$\begin{array}{cl}
\left\{\begin{array}{c}—\\—\end{array}\right\} & \begin{array}{l} 0.92|2\overline{\tfrac{3}{2}}\rangle + 0.36|\bar{1}\overline{\tfrac{3}{2}}\rangle + 0.10|1\overline{\tfrac{1}{2}}\rangle \\ 0.92|\bar{2}\tfrac{3}{2}\rangle - 0.36|1\tfrac{3}{2}\rangle + 0.10|\bar{1}\tfrac{1}{2}\rangle \end{array} \\
\left\{\begin{array}{c}—\\—\end{array}\right\} & \begin{array}{l} -0.82|\bar{2}\tfrac{1}{2}\rangle - 0.45|2\overline{\tfrac{1}{2}}\rangle + 0.25|1\tfrac{1}{2}\rangle - 0.20|\bar{1}\overline{\tfrac{1}{2}}\rangle - 0.10|\bar{3}\tfrac{3}{2}\rangle \\ -0.87|2\overline{\tfrac{1}{2}}\rangle + 0.35|\bar{2}\tfrac{1}{2}\rangle - 0.28|\bar{1}\overline{\tfrac{1}{2}}\rangle - 0.20|1\tfrac{1}{2}\rangle - 0.10|3\overline{\tfrac{3}{2}}\rangle \end{array} \\
\left\{\begin{array}{c}—\\—\end{array}\right\} & \begin{array}{l} -0.94|\bar{2}\overline{\tfrac{1}{2}}\rangle + 0.32|1\overline{\tfrac{1}{2}}\rangle - 0.10|\bar{3}\tfrac{1}{2}\rangle \\ 0.94|2\tfrac{1}{2}\rangle + 0.32|\bar{1}\tfrac{1}{2}\rangle + 0.10|3\overline{\tfrac{1}{2}}\rangle \end{array} \\
\left\{\begin{array}{c}—\\—\end{array}\right\} & \begin{array}{l} 0.95|\bar{2}\overline{\tfrac{3}{2}}\rangle - 0.30|1\overline{\tfrac{3}{2}}\rangle + 0.10|\bar{3}\overline{\tfrac{1}{2}}\rangle \\ -0.95|2\tfrac{3}{2}\rangle - 0.30|\bar{1}\tfrac{3}{2}\rangle - 0.10|3\tfrac{1}{2}\rangle. \end{array}
\end{array}$$

The corresponding paramagnetic susceptibility is equal to:

$$\begin{aligned}\chi_M = {} & [(5.60/T + 0.0095) + (1.78/T + 0.0039)\exp(-360/T) \\ & + (0.12/T - 0.0027)\exp(-720/T) + (0.47/T - 0.0106)\exp(-1080/T)] \\ & \times [2 + 2\exp(-360/T) + 2\exp(-720/T) + 2\exp(-1080/T)]^{-1}.\end{aligned}$$

Co^{2+}, C_{4v}

A system of two Kramers doublets with a gap between them of ca. 100 K is assumed as the ground state:

$$\left\{\begin{matrix}— \\ —\end{matrix}\right\}\begin{matrix} 0.72|\bar{2}\overline{\tfrac{3}{2}}\rangle + 0.67|2\overline{\tfrac{3}{2}}\rangle + 0.15|1\overline{\tfrac{1}{2}}\rangle \\ 0.72|2\tfrac{3}{2}\rangle + 0.67|\bar{2}\tfrac{3}{2}\rangle + 0.15|\bar{1}\tfrac{1}{2}\rangle \end{matrix}$$

$$\left\{\begin{matrix}— \\ —\end{matrix}\right\}\begin{matrix} 0.69|\bar{2}\overline{\tfrac{1}{2}}\rangle + 0.68|2\overline{\tfrac{1}{2}}\rangle + 0.16|1\tfrac{1}{2}\rangle + 0.15|\bar{1}\overline{\tfrac{3}{2}}\rangle \\ 0.69|2\tfrac{1}{2}\rangle + 0.68|\bar{2}\tfrac{1}{2}\rangle + 0.16|\bar{1}\overline{\tfrac{1}{2}}\rangle + 0.15|1\tfrac{3}{2}\rangle. \end{matrix}$$

Its paramagnetic susceptibility is:

$$\begin{aligned}\chi_M = {} & [(2.92/T + 0.0412) + (2.31/T - 0.0412)\exp(-100/T)] \\ & \times [2 + 2\exp(-100/T)]^{-1}.\end{aligned}$$

The above expressions describe the average molar susceptibility ($\frac{1}{3}\chi_M{}^{\parallel} + \frac{2}{3}\chi_M{}^{\perp}$) neglecting the constant terms of polarizing contribution of unpopulated levels, which do not exceed 500×10^{-6} emu.

The formula for the magnetic susceptibility of Ni^{2+} and Co^{2+} ions in the cubic crystal fields O_h and T_d have been given previously by Kotani (*19*), Griffith (*20, 21*), Figgis (*22*) and Lotgering (*23*). Theoretical ($\chi_M{}^{-1}$, T) plots for these two coordinations, presented in Figs. 2, 3, 4, and 5, were calculated on the basis of the papers cited above. The following values were used for these calculations: for Ni^{2+} ion $\lambda = -250$ cm^{-1}, 10 $Dq = 8600$ cm^{-1} in octahedral field (*24*), 10 $Dq = 4650$ cm^{-1} and $\tau^2 = 0.013$ in tetrahedral field (*25*); for Co^{2+} ion $\lambda = -150$ cm^{-1}, 10 $Dq = 10230$ cm^{-1}, and $\tau^2 = 0.04$ in octahedral field (*26*), 10 $Dq = 4000$ cm^{-1} in tetrahedral field (*25*). τ is the ${}^3F$–${}^3P$ and ${}^4F$–${}^4P$ admixing coefficient for Ni^{2+} and Co^{2+} ions, respectively.

REFERENCES

1. Broussard, L., and Shoemaker, D. P., *J. Amer. Chem. Soc.* **82**, 1041 (1960).
2. Olson, D. H., *J. Phys. Chem.* **72**, 4366 (1968).
3. Gallezot, P., and Imelik, B., *J. Phys. Chem.* **77**, 652 (1973).
4. Riley, P. E., and Seff, K., *J. Chem. Soc. Chem. Commun.* **23**, 1287 (1972).
5. Heilbron, M. A., and Vickerman, J. C., *J. Catal.* **33**, 434 (1974).
6. Mikheikin, I. D., Brotikovskii, O. I., Zhidomirov, G. M., and Kazanskii, V. B., *Kinet. Katal.* **12**, 1442 (1971).
7. Rabo, J. A., Angell, C. L., Kasai, P. H., and Schomaker, V., *Discuss. Faraday Soc.* **41**, 328 (1966).
8. Wichterlova, B., Jiru, P., and Curinova, A., *Z. Phys. Chem. Neue Folge No.* **1–4**, 180 (1974).
9. Klier, K., *J. Amer. Chem. Soc.* **91**, 5392 (1969).
10. Klier, K., and Ralek, M., *J. Phys. Chem. Solids* **29**, 951 (1968).
11. Egerton, T. A., Hagan, A., Stone, F. S., and Vickerman, J. C., *J. Chem. Soc. Faraday Trans. I* **68**, 723 (1972).
12. Egerton, T. A., and Vickerman, J. C., *J. Chem. Soc. Faraday Trans. I* **69**, 39 (1973).
13. Bremer, H., Schoedel, R., Vogt, F., Rubinshtein, A. M., Slinkin, A. A., and Fedorovskaya, G. A., *Z. Chem.* **13**, 350, Heft 9 (1973).
14. Smith, *J. V.*, *Advan. Chem. Ser.* **101**, 171 (1971).
15. Breck, D. W., "Zeolite Molecular Sieves." Wiley, New York, 1974.
16. Smith, J. V., and Dowell, L. G., *Z. Kristallogr.* **126**, 135 (1968).
17. Gallei, E., Eisenbach, D., and Ahmed, A., *J. Catal.* **33**, 62 (1974).

18. Breck, D. W., "Zeolite Molecular Sieves." Chap. 6, p. 441. Wiley, New York, 1974.

19. Kotani, M., *J. Phys. Soc. Japan* **4**, 293 (1949).

20. Griffith, J. S., *Trans. Faraday Soc.* **54**, 1109 (1958).

21. Griffith, J. S., "The Theory of Transition Metal Ions," Chap. 10. Univ. Press, Cambridge, 1961.

22. Figgis, B., *Nature* (London) **182**, 1568 (1958).

23. Lotgering, F. K., *J. Phys. Chem. Solids* **23**, 1153 (1962).

24. Low, W., *Phys. Rev.* **109**, 247 (1958).

25. McClure, D. S., *J. Phys. Chem. Solids* **3**, 315 (1957).

26. Low, W., *Phys. Rev.* **109**, 256 (1958).